# Dependence of Air Quality in a Remote Location on Local and Mesoscale Transports: A Case Study

JOHN J. CARROLL AND RONALD L. BASKETT[1]

*Department of Land, Air and Water Resources, University of California, Davis 95616*

(Manuscript received 28 July 1978, in final form 4 January 1979)

ABSTRACT

The results of a field study utilizing ground-based and aircraft measurements of meteorological parameters and several air pollutants are described for two summer periods in the vicinity of Yosemite National Park, California. These results are related to observed air quality and atmospheric circulation patterns in neighboring parts of the state and to transport by the local mountain-valley wind system. The conclusion is reached that maximum air quality degradation in the study area does not occur during persistent periods of large-scale stagnation, but occurs as the result of transport from area sources up to 200 km away by the typical extended sea breeze circulation which develops following such a period.

## 1. Introduction

This paper summarizes a field study undertaken to examine the degree to which air quality in Yosemite Valley depends on locally generated as opposed to imported air pollutants. The primary purpose of this effort was to provide local authorities with an estimate of the improvement one could expect in local air quality with implementation of a local emission control strategy. The theme of this paper is to examine the interaction of synoptic-scale through local-scale flow patterns as related to the effective transport of air pollutants to the subject area. A more detailed discussion of the study is contained in Baskett (1976). While the following discussion is area-specific, it serves as an illustration of the role of the sequential development of meteorological conditions and related transport phenomena in determining the air quality of an area relatively free of combustive sources.

A map of central California is presented in Fig. 1 which gives the location of various landmarks and measurement sites referred to in this paper. Also shown is the typical summer afternoon wind field characterized by an extended sea breeze flow through the San Francisco Bay Area (SFBA) to the Central Valley and upslope flow over the western face of the Sierra Nevada Mountains. The detailed characteristics of this flow, and its climatology and capacity for transporting primary and secondary pollutants away from the highly urbanized SFBA, have been discussed in a number of papers (Angell *et al.*, 1966; Miller *et al.*, 1972; Miller and Ahrens, 1970; Schroeder *et al.*, 1967; Fosberg and Schroeder, 1966; Schroeder, 1961; Frenzel, 1962).

The development of the extended sea breeze depends on the position of the eastern Pacific subtropical high pressure cell and on the upper level wave pattern as represented by the 500 mb pressure surface. With cyclonic curvature aloft, the surface high is farther west from the coast, resulting in weaker subsidence over the state, a stronger onshore pressure gradient and a more strongly developed onshore flow. Under these conditions, the depth of the mixed layer is fairly small throughout the area in Fig. 1, since the combined effect of the weak subsidence and the marine air intrusion is to maintain an inversion within 1 km of the surface. This inversion is lower at night than during the day and is generally lower at the coast than inland. Therefore, the observed minimum air quality degradation in urban areas during such periods is the result of higher surface wind speeds rather than increased vertical dispersion. From the typical summer wind field, calculated average trajectories show that parcels initially located over San Francisco at either 1200 or 2400 PST would arrive at the base of the Sierras west of Yosemite Valley 16 h later (Frenzel, 1962).

With anticyclonic curvature aloft, the surface high-pressure centers are normally located north or northeast of the State. In these situations, strong subsidence occurs, the onshore pressure gradient is reduced or reversed, and the coastal and inland areas experience strong low-level inversions, light and variable winds, high surface temperatures and maximum air quality degradation.

In the absence of a strong synoptic-scale pressure

[1] Present affiliation: Environmental Research and Technology, Inc., Westlake Village, CA 91361.

0021-8952/79/040474-13$07.25

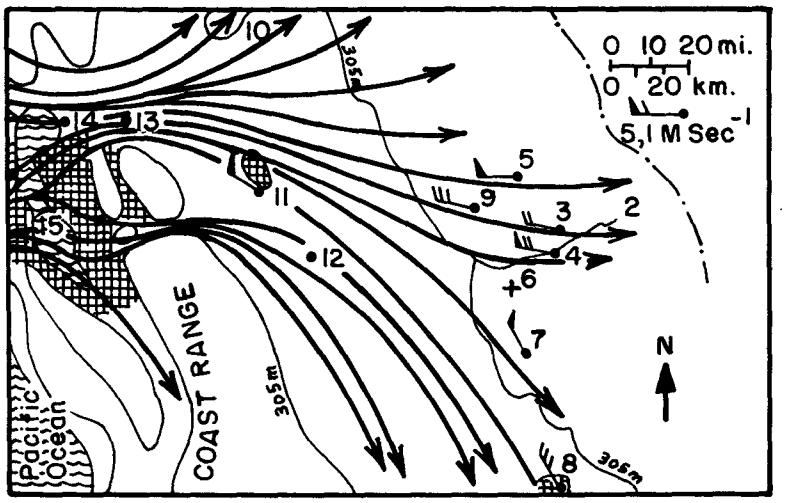


FIG. 1. Map of central California showing general topography (305 m contour), major urban areas (cross hatching), average summer afternoon (1600 PST) surface wind field, and locations referred to in this paper: 1, dot-dashed line marking the Sierra Crest (east-west divide); 2, Yosemite Valley; 3, Crane flat; 4, El Portal; 5, Woodsridge; 6, Mariposa Airport; 7, Green Mountain; 8, Fresno; 9, Groveland; 10, Sacramento; 11, Stockton; 12, Modesto; 13, Pittsburg; 14, Vallejo; 15, San Francisco Bay Area.

gradient, typically the case in summer, the flow over the western slope of the Sierra is characterized by well-developed mountain-valley wind systems. The orientation of the general slope and of the valleys that drain into the Central Valley is optimal for the development of such flows (cf. Cramer and Lynott, 1961; Ayers, 1961; Gleeson, 1953; Fleagle, 1950). The typical daily cycle of these flows near the Central Valley and their relation to the extended sea breeze flow is illustrated by the wind data from Green Mountain summarized in Fig. 2 (Schultz, 1974). For simplicity, only the northerly components—which include more than 70% of all observations—are shown. The data for both months exhibit the same general features, *viz.*, early morning downslope flow (northeast-east) at approximately 1.5 m $s^{-1}$; upslope flow through the middle of the day (west-northwest) at 3–5 m $s^{-1}$; and the extended sea breeze from mid-afternoon through midnight (north-northwest to north-northeast) also at 3–5 m $s^{-1}$ but with a wind shift. The probability of the extended sea breeze replacing the afternoon upslope flow decreases with distance upslope from the Central Valley.

The distribution, intensity and nature of the pollutant sources along the average sea breeze trajectory vary considerably. The SFBA has extensive resi-

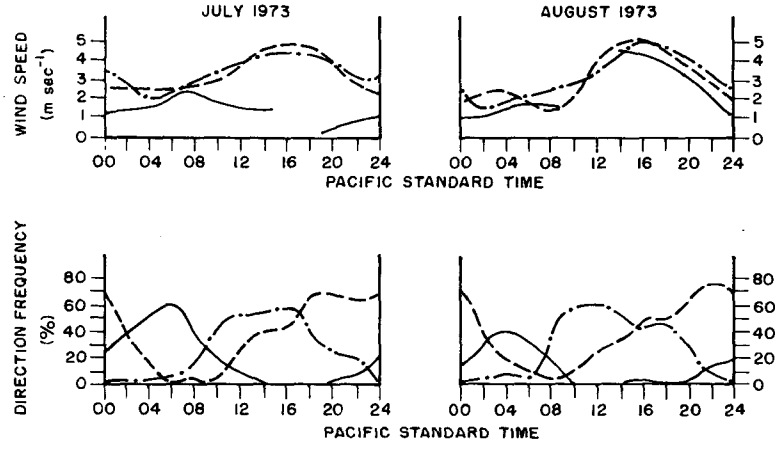


FIG. 2. Average wind speed and directional frequency by intervals versus time of day for July and August 1973 at Green Mountain. Solid lines represent winds between east and northeast, dashed lines between north-northwest and north-northeast and dot-dashed lines between west and northwest (after Schultz, 1974).

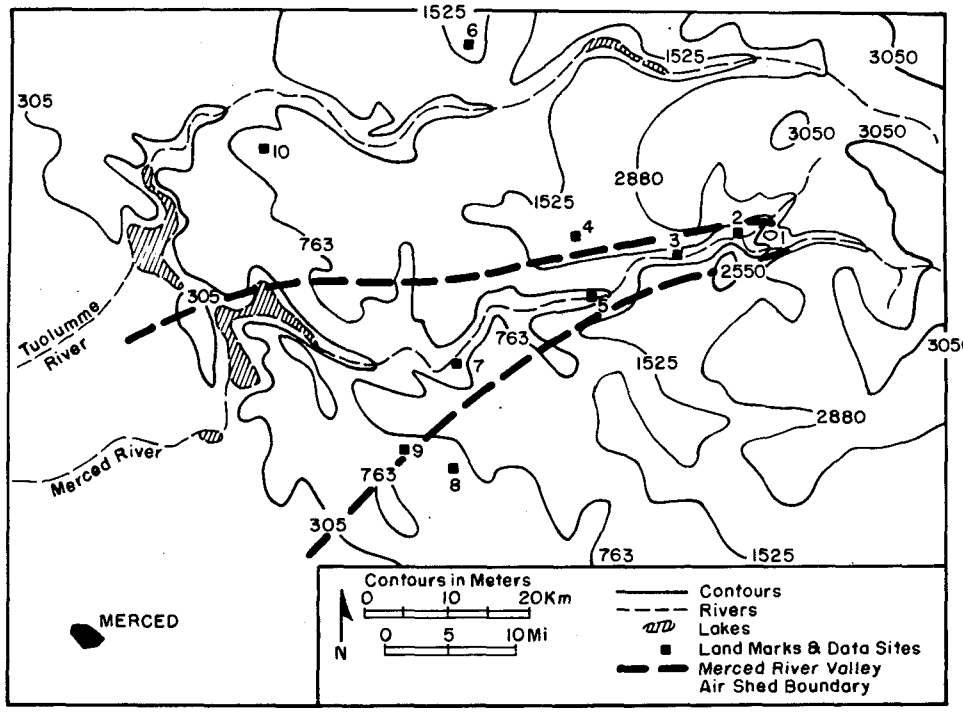


FIG. 3. Map of the subject area showing smoothed topography, airshed boundary (heavy dashed lines), data sites and major landmarks: 1, Half Dome; 2, Stoneman Meadows; 3, El Capitan Meadows; 4, Crane Flat; 5, El Portal; 6, Woodsridge; 7, Briceburg; 8, Mariposa; 9, Mariposa Airport; 10, Groveland.

dential, commercial, transportation and industrial sources—including petrochemical facilities. Historically, sulfur emissions have been relatively low with oxidant smog dominant. Within the gaps in the Coastal Range and in the Central Valley, the major sources are several urban, lightly industrialized areas, major transportation corridors and the burning of agricultural residues. The former sources contribute additional reagents for oxidant smog formation; the latter appears to cause mostly visibility degradation.

Since the summer inversions are present over most of the area most of the time, vertical dispersion is limited. Since strong subsidence generally precludes development of the extended sea breeze, air quality in the vicinity of these area and line sources is extremely poor when this condition occurs. With the return of the extended sea breeze following such an episode, high pollutant concentrations could be advected to the Sierra foothills and be available for transport upslope. The field study summarized in the following sections was designed in part to verify this scenario by measuring the relevant meteorological parameters and several air pollution constituents in and above the general vicinity of Yosemite National Park and by relating these to the larger scale flow patterns and air pollution concentrations upwind of the study area.

## 2. Experimental methodology

A detailed map of the subject area is presented in Fig. 3. Periodic ground-level measurements were made at Mariposa Airport, and at El Capitan and Stoneman Meadows within the Yosemite Valley in conjunction with the operation high-volume particle collectors. At the two Yosemite Valley sites, single theodolite pilot balloon observations were made to determine wind flow from the valley floor to a height ~500 m above the top of the valley walls. In addition, a total oxidant meter (Mast Model 724-2) was operated at the El Capitan site. Wind observations taken twice per day by fire prevention services are also available for Crane Flat, El Portal, Woodsridge and Groveland (cf. Fig. 3). These measurements provide information on the temporal variations at fixed points at or near the surface. To obtain continuous spatial measurements and information on the vertical distribution of pollutants and their relation to atmospheric stability, aircraft-based observations were made over the area bounded by the heavy dashed lines shown in Fig. 3. The aircraft was a Cessna 336 equipped with the instrumentation shown in Fig. 4.

Standard techniques were used in the measurement of all meteorological variables with the exception of humidity. The aircraft hygrometer unit (ERC Model BLR) measures the attenuation of Lyman-alpha radiation (0.12156 mm) in a short, open path between

a regulated source and a detector. With the assumption that all attenuation is due to absorption by hydrogen atoms and since essentially all hydrogen in the path is associated with water vapor, the attenuation is proportional to the water vapor density in the sample volume. With the particle collection and counting system shown in Fig. 4, average number concentrations for any sampling period is determined by the optical counter which detects ~90% of particles with equivalent scattering diameters $\gtrsim 0.3$ μm. Size distributions for contemporaneous samples are obtained by manual counting of optically magnified sections of the cellulose filters (Millipore, type HA) using Nomarski differential interference optics.

The aircraft ozone meter measures the differential absorption of ultraviolet radiation between samples of ambient air which alternately pass through or around an ozone trap. Therefore, the measurements are relatively free of interference and the output is proportional to the ozone density in the sample volume. The factory calibration for these units, however, is given in terms of ozone mixing ratio (pphm) at normal ambient conditions (101.3 Pa, 20°C). Therefore, at lower pressures or higher temperatures, the displayed output underestimates the actual ozone mixing ratio. For example, with a change in elevation from sea level to 3000 m, air density decreases ~25% and the actual ozone mixing ratio at that altitude would be ~25% greater than that indicated by the instrument. Due to the complexity of calculating individual corrections for each data point, the aircraft ozone data presented in the following section are *not* corrected for nonstandard air density.

The ground-level particle collectors were four-stage Lundgren-type sequential drum impactors fitted with membrane afterfilters (Nucleapore, 0.1 μm pore size). Since impactor collection efficiency is variable and difficult to document in field situations, we assume that the last stage ($0.5 \lesssim d \lesssim 2$ μm) is 50% efficient and that nearly all particles $>2$ μm equivalent diameter are collected somewhere in the impactor. We also assume that all particles $\gtrsim 0.1$ μm diameter are collected by the impactor-afterfilter system. These particle samples were analyzed for elemental composition, stage by stage using an alpha-particle-excited, x-ray emission technique developed at the UCD Crocker Nuclear Laboratory. The technique allows determination of the mass of individual chemical elements (heavier than sodium) whose concentration is greater than a threshold value. This detection theshold depends on the collection substrate material, detector sensitivity and the total mass loading on the target. Therefore, the detection threshold for any element varies from stage to stage in the impactor samples, from sample period to sample period and from impactor to afterfilter samples.

Field observations were made during two periods, 25–27 July and 29–30 August 1973, between the hours of 0600 and 1600 PST. Surface wind, oxidant and pibal data were taken hourly. The aircraft flights, of approximately 1.5 h duration, were performed at times nominally centered on 0730, 1030 and 1400 PST. The surface particle collectors were operated to obtain individual samples of 2 h duration centered on the aircraft flight times.

Aircraft operations were based at Mariposa Airport. For all flights, the ascending flight path was initially westward to a point over the Central Valley ~30 km west of the airport. The aircraft then turned eastward continuing to climb until past Half Dome, where the

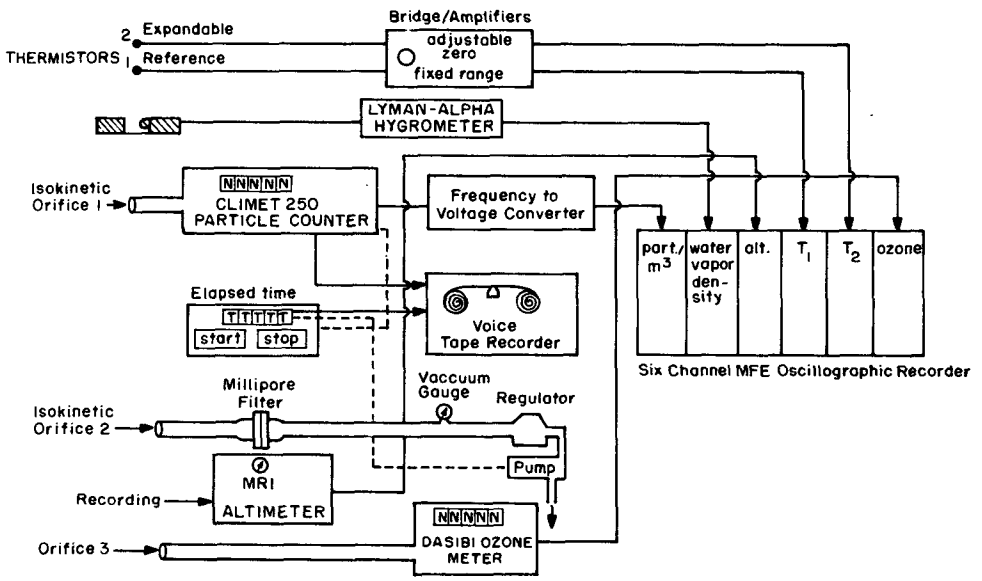


FIG. 4. Schematic diagram of the aircraft instrumentation system.

particle collection filter was changed, the ascending data set was closed and the descending data set was initialized. A lower altitude descent was then made westward, following the same ground track. Horizontal position was correlated with the temporal information on the recorder by the use of frequent visual bearings to landmarks along the visually aligned flight paths. From these references and the recorded altitude, cross sections of temperature, water vapor density and uncorrected ozone mixing ratio were constructed. While these data are not simultaneous, a measure of the temporal variation occurring during the flight is available since the descending flight path crosses the ascending path west of the airport. Temperature was the only variable that showed significant variations, in which case average lapse rates, stable layer positions and temperatures are used to construct the cross sections.

It was hoped that the linear array of surface particle collectors would provide a measure of the surface gradient of elements that are indicative of anthropogenic sources such as lead as an indicator of automobile traffic. Temporal variation in these gradients coupled with the observed wind field would allow calculation of advective transport rates. In practice, however, the elemental analysis for the surface particulate samples showed that most of these particles are composed of local soil elements with sulfur being the only element detected at significant levels which might be anthropogenic in origin. A number of more sensitive tests for lead were performed but without reliable results. Therefore, the only "tracers" available to document inferred transport are the ozone distribution above the surface, the oxidant concentrations at El Capitan and the surface concentration of particle-borne sulfur.

We note here that use of these substances as tracers is subject to several constraints which preclude rigorous quantitative documentation of transport rates. However, by allowing for the known behavior of these pollutants, the occurrence of significant transport can be clearly demonstrated. These constraints are of two general types: uncertainty in the type and location of the sources of the measured substance, and the dependence of locally measured concentration on chemical and atmospheric dynamics as well as on reagent emission rates.

For total oxidant or ozone, the second constraint is of major importance since, in general, anthropogenic activity is the primary source of reagents whenever local concentrations exceed a few parts per hundred million. For a given source strength and a fixed air volume, the locally measured ozone concentration depends on the relative rates of production and destruction of $O_3$. The production rate depends on the availability of solar radiation and on the concentration of reagents, primarily $NO_x$ and gaseous hydrocarbons. The destruction rate depends on the availability of internal reducing media (suspended particles), internal chemical sinks and the rate of diffusive transport to reducing media at the ground. Since the destruction mechanisms become increasingly effective with increasing atmospheric turbulence, higher destruction rates are expected with increasing wind speeds and thermal convection. Since increasing wind speeds and turbulence also mean increasing air volume and greater mixed-layer depths, the production rate for constant source strength will decrease. Therefore, given steady-state source strengths, locally measured $O_3$ concentrations should vary inversely with near-ground wind speed and the intensity of thermal convection.

For sulfur, both constraints are important. In biologically active areas, such as that studied, significant emissions of sulfur ($H_2S$) are naturally present and exceed local anthropogenic sources. The chemical processes leading to formation of particulate sulfur compounds at low relative humidities are not well understood. However, in an oxidizing atmosphere, the formation of such particles appears to occur fairly rapidly and these compounds, once formed, appear to be stable. Therefore, variations in concentrations of sulfur in particulate form can be used as indicators of transport if local contributions can be estimated.

## 3. Observational results

Both operational periods began at a time when the extended sea breeze circulation had been absent for the previous day or longer. For the July period, strong subsidence and light and variable winds persisted through the 26th with a weaker than average sea breeze developing on the 27th. In August the extended sea breeze developed on both days following a period of stagnation similar to that in the period 25–27 July. As a result high concentrations of primary and secondary pollutants were present over the SFBA and over parts of the Central Valley at the beginning of both periods. In Table 1, the maximum hourly averaged concentrations of pollutants for the calendar days immediately before and during the observational periods is given for several central California monitoring stations. Note that at most of these stations, the maximum hourly concentrations of oxidant and $NO_x$ observed for the month was equaled during or immediately before the operational periods and that maxima at the interior stations occur one or two days after maxima at the coastal stations.

In the absence of a strong synoptic-scale pressure gradient the diurnal cycle of mountain-valley winds developed over the Sierra slopes during both periods. The average characteristics of these flows, as derived from all available wind data in the vicinity of the study area, are tabulated in Table 2. From these statistics, an estimated wind passage for a point on the slope similar to Yosemite Valley was calculated

TABLE 1. Maximum hourly concentration (pphm) of pollutants in central California for calendar days indicated (California Air Quality Data, Vol. 5, No. 3).

| Place and pollutant | | July 24 | 25 | Period of operation 26 | 27 | Maximum for Month | August 27 | 28 | Period of operation 29 | 30 | Maximum for Month |
|---|---|---|---|---|---|---|---|---|---|---|---|
| San Francisco (downtown) | CO | 500 | 900 | 700 | — | 900 | 200 | 500 | 300 | 200 | 600 |
| | OX | 3 | 4 | 3 | 5 | 5 | 1 | 5 | 1 | — | 5 |
| | $NO_x$ | 21 | 40 | 27 | 11 | 40 | 12 | 47 | 25 | 14 | 47 |
| | HC | 300 | 700 | 300 | 300 | 700 | 300 | 700 | 400 | 300 | 700 |
| Vallejo | CO | 400 | 500 | 500 | 400 | 500 | 300 | 600 | 400 | 300 | 600 |
| | OX | 8 | 12 | 14 | 6 | 14 | 4 | 8 | 5 | 2 | 9 |
| | $NO_x$ | 8 | 14 | 12 | 7 | 16 | 6 | 16 | 14 | 4 | 18 |
| | HC | 200 | 500 | 400 | 200 | 500 | 200 | 600 | 500 | 100 | 600 |
| Pittsburg | CO | 500 | 600 | 300 | 200 | 600 | 300 | 500 | 400 | 300 | 500 |
| | OX | 5 | 8 | 7 | 7 | 8 | 3 | 8 | 7 | 3 | 10 |
| | $NO_x$ | 7 | 14 | 16 | 4 | 16 | 7 | 10 | 12 | 7 | 12 |
| | HC | 300 | 600 | 600 | 200 | 600 | 300 | 500 | 600 | 300 | 600 |
| Stockton | CO | 200 | 400 | 500 | 100 | 500 | 200 | 300 | 400 | 100 | 400 |
| | OX | 11 | 18 | 13 | 10 | 18 | 7 | 8 | 16 | 14 | 16 |
| | $NO_x$ | 8 | 23 | 21 | 10 | 27 | 6 | 18 | 19 | 19 | 22 |
| | HC | 400 | 700 | 700 | 300 | 700 | 400 | 800 | 700 | 300 | 1500 |
| Modesto | CO | 200 | 300 | 200 | 200 | 300 | 200 | 300 | 600 | 200 | 600 |
| | OX | 10 | 14 | 17 | 15 | 17 | 8 | 11 | 16 | 9 | |
| | $NO_x$ | 8 | 15 | 8 | 7 | 18 | 7 | 13 | 19 | 11 | 23 |
| | HC | 400 | 700 | 600 | 400 | 700 | 300 | 400 | 700 | 400 | 700 |

and is also tabulated. Since these winds tend to remain within 300 m of the surface and are channeled by local topography, the net wind passage is essentially equivalent to the average net transport distance per day within the Merced River Valley as a whole. Since Yosemite Valley is ~120 km upstream from the Central Valley, air from the Central Valley should reach Yosemite Valley by midafternoon on an average day. For the July period, the measured winds show that the afternoon valley wind began about an hour later and was 15% weaker than average. In August, the afternoon valley wind was observed an hour earlier and was ~5% stronger than the average.

TABLE 2. Typical characteristics of the summer mountain-valley winds in the vicinity of Yosemite National Park.

| Nomenclature | Average speed (upslope>0) (m $s^{-1}$) | Time of occurrence (PST) | Upslope wind passage (km) |
|---|---|---|---|
| Mountain wind | −1.5 | 2300–0700 | −42 |
| Morning valley wind | 2.0 | 0700–1100 | +30 |
| Afternoon valley wind | 5.0 | 1100–1700 | +108 |
| Evening valley wind | 3.0 | 1700–2000 | +30 |
| Transition | ~0 | 2000–2300 | ~0 |
| Net passage per day | — | — | 126 |

The measured concentrations of particle-borne sulfur are summarized in Table 3. The fact that the detection threshold is much higher for the membrane filter samples is reflected by the sparsity of data for the total system. Where such data are available, we note that the ratio of impacted sulfur to impacted plus filter-collected sulfur is not constant among samples, suggesting that the size distribution of the sulfur-bearing particles or the impactor collection efficiency varies significantly among samples. In any case, the maximum measured concentrations in July are less than 0.4 $\mu$gm $m^{-3}$ where, as in August, maxima in excess of 1.6 $\mu$gm $m^{-3}$ were found. Also, there is an indication that total concentration at all stations increases from morning to afternoon. Surface oxidant measurements (as shown in Fig. 5) also show concentrations increasing to an afternoon maximum and that in August the maxima are greater than in July.

Vertical cross sections of temperature, water vapor density and uncorrected ozone mixing ratio are presented in Figs. 6, 7 and 8 for 26 July, 29 and 30 August, respectively. Vertical time sections of wind over the western part of the Yosemite Valley are shown in Fig. 9 for the same days. Average particle concentrations along the aircraft flight paths are summarized in Table 4. The July data represent a stagna-

TABLE 3. Concentrations of sulfur ($\mu g\ m^{-3}$) in particles from impactor samples ($D \gtrsim 0.5\ \mu m$) and from impactor plus after-filter samples ($D \gtrsim 0.1\ \mu m$) for times and places shown.

| Date | Mean time (PST) | Mariposa | | El Capitan | | Stoneman | |
|---|---|---|---|---|---|---|---|
| | | $D \gtrsim 0.5\ \mu m$ | $D \gtrsim 0.1\ \mu m$ | $D \gtrsim 0.5\ \mu m$ | $D \gtrsim 0.1\ \mu m$ | $D \gtrsim 0.5\ \mu m$ | $D \gtrsim 0.1\ \mu m$ |
| 25 Jul | 1700 | — | — | 0.093 | — | — | — |
| 26 Jul | 0930 | — | — | 0.068 | — | 0.081 | — |
| | 1230 | 0.159 | — | 0.160 | — | 0.118 | — |
| | 1600 | — | — | 0.174 | — | 0.214 | 0.379 |
| 27 Jul | 0800 | 0.129 | 0.300 | — | — | — | — |
| | 1030 | 0.190 | 0.335 | 0.219 | — | — | — |
| 29 Aug | 0900 | 0.111 | 0.570 | 0.062 | 0.588 | 0.069 | 0.777 |
| | 1200 | 0.174 | 0.841 | 0.107 | — | 0.087 | — |
| | 1500 | 0.225 | 1.610 | 0.114 | 1.246 | 0.092 | — |
| 30 Aug | 0900 | 0.153 | 1.066 | 0.150 | — | 0.075 | — |
| | 1130 | 0.175 | 0.987 | 0.105 | — | 0.107 | 0.618 |
| | 1430 | 0.200 | — | 0.124 | 0.794 | 0.110 | 1.665 |

tion case in which stong subsidence maintains a shallow mixed layer near the ground, precludes development of the extended sea breeze and inhibits the development of the afternoon valley wind. As a result, primary and secondary pollutants remain in the general vicinity of the source areas, except close to the foothills where some upslope advection by the weaker than average valley wind occurred. The August case represents the situation in which regional-scale advection occurs following a period of stagnation. Lapse rates in the stable layers ranged from isothermal to 1.4°C $(100\ m)^{-1}$. Within a given layer the stability is greatest over the central valley. Maximum stability on any day was observed during the second flight (1000 to 1130 PST) and the highest lapse rate observed among all days was on 26 July in the upper inversion over the Central Valley during the second flight.

The temperature and humidity data for 26 July illustrate the persistence of strong susbidence over the region. In particular, the inversion bases actually lowered during the day, in spite of strong surface heating and were still present close to the mountain slopes in midafternoon. As a result of the limited vertical dispersion over the Central Valley and reduced upslope transport, air quality over the lower elevations degraded slowly during the day, while above 1500 m the air quality remained good, with $O_3$ concentrations remaining below 10 pphm. The data for this day are interpreted as indicative of the degree to which local sources degrade local air quality under extremely adverse dispersion conditions. We also note that $O_3$ concentrations observed in the study area are considerably lower than the maximum hourly averages in Modesto on the same day or Stockton on the previous day (cf. Table 1).

In contrast, the August observations were made during a period in which subsidence was weaker, an average sea breeze developed and the daytime valley winds were stronger than the average. We also note that on 28 August a weak extended sea breeze developed by late afternoon. The observed thermal structure in August is more complex and its temporal variation differs in several significant ways from the July case. As the day progresses, the depth of the surface mixed layer increases and the inversions do not persist close to the lower slopes through midafternoon. The slope of the isotherms near the mountain slopes is greater (downward to the west) which is a necessary condition for stronger upslope flow. The change in water vapor distribution with time is in the sense of upslope flow over the foothills and sinking over the Central Valley.

The most striking difference between the two periods is with the concentration and distribution of ozone. The larger, early morning maximum (>24 pphm) observed over and west of Mariposa Airport on the 29th occurred within the lower inversion and is probably due to a moderate production rate and a very low destruction rate in reagents transported partially upslope the previous evening and downslope in the predawn hours. As the second sounding shows, the maximum did not persist as increasing surface winds

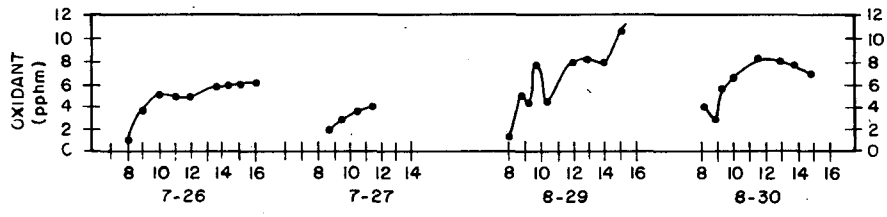


FIG. 5. Total ground-level oxidant concentrations at El Capitan.

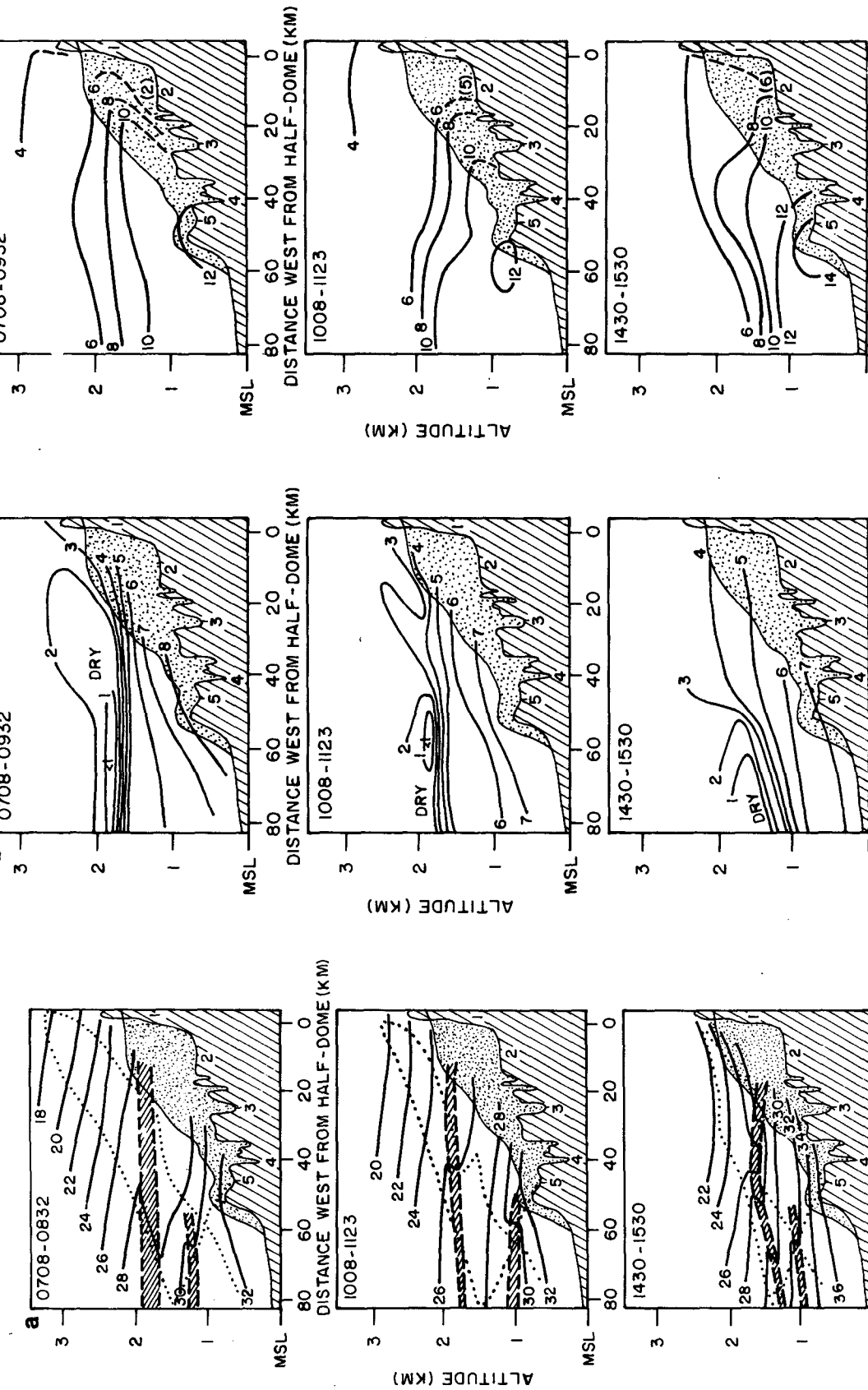


FIG. 6a. Vertical cross section of temperature for 26 July 1973 over the lower Merced River watershed. Lower light line represents topography along line from Half Dome through Yosemite Valley and Briceburg to the Central Valley. Upper light line represents smoothed topography at the watershed boundary (heavy dashed line in Fig. 4). Landmarks identified are 1, Half Dome; 2, Yosemite Valley; 3, El Portal; 4, Briceburg; 5, Mariposa Airport. The dotted line represents the aircraft flight path as projected onto the $x$-$z$ plane. Isothermal or inversion layers are bounded by dashed lines and shaded.

FIG. 6b. Cross section of water vapor density ($10^{-6}$ gm cm$^{-3}$) for 26 July 1973.

FIG. 6c. Cross section of uncorrected ozone mixing ratio (ppbm) for 26 July 1973.

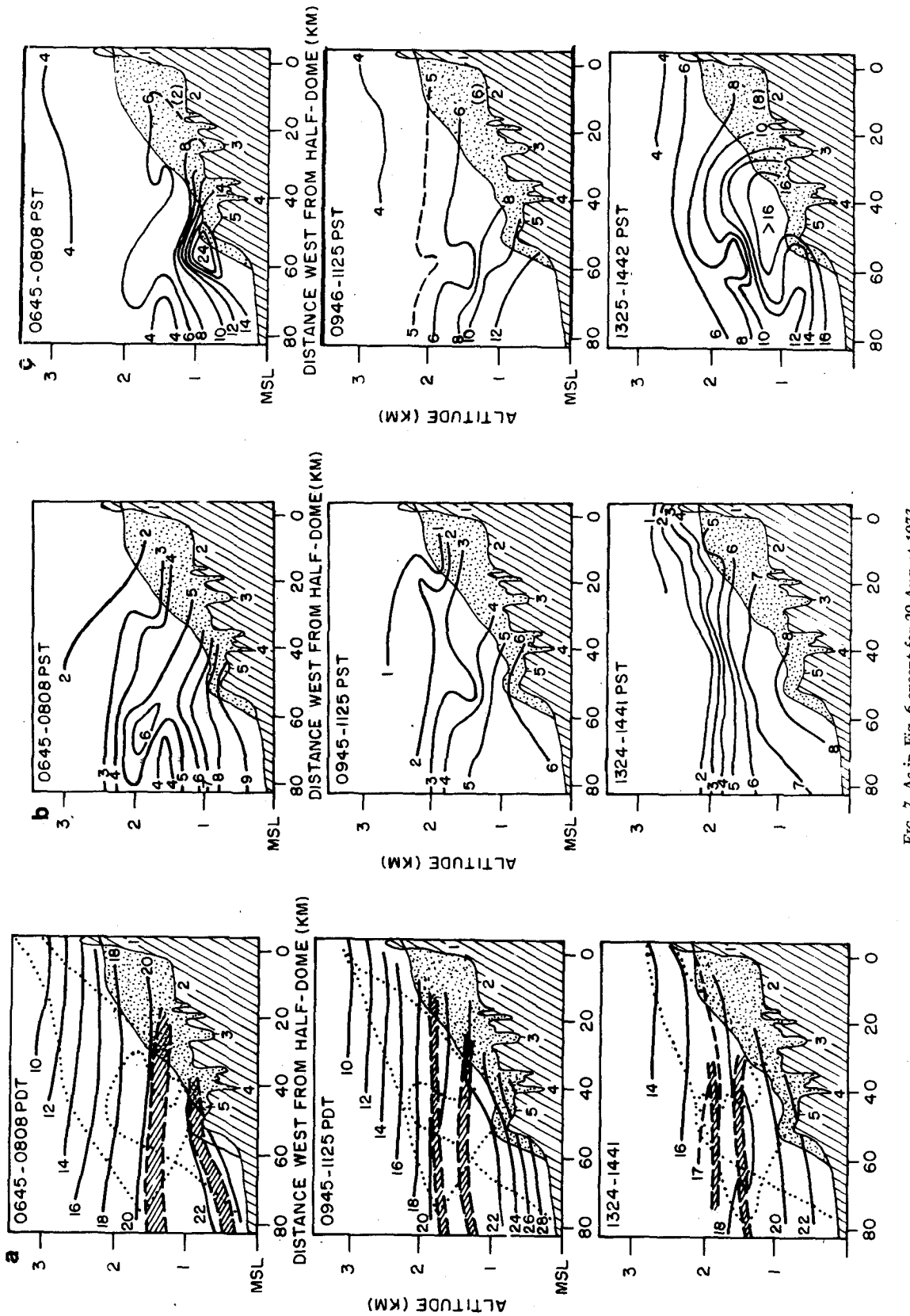


FIG. 7. As in Fig. 6 except for 29 August 1973.

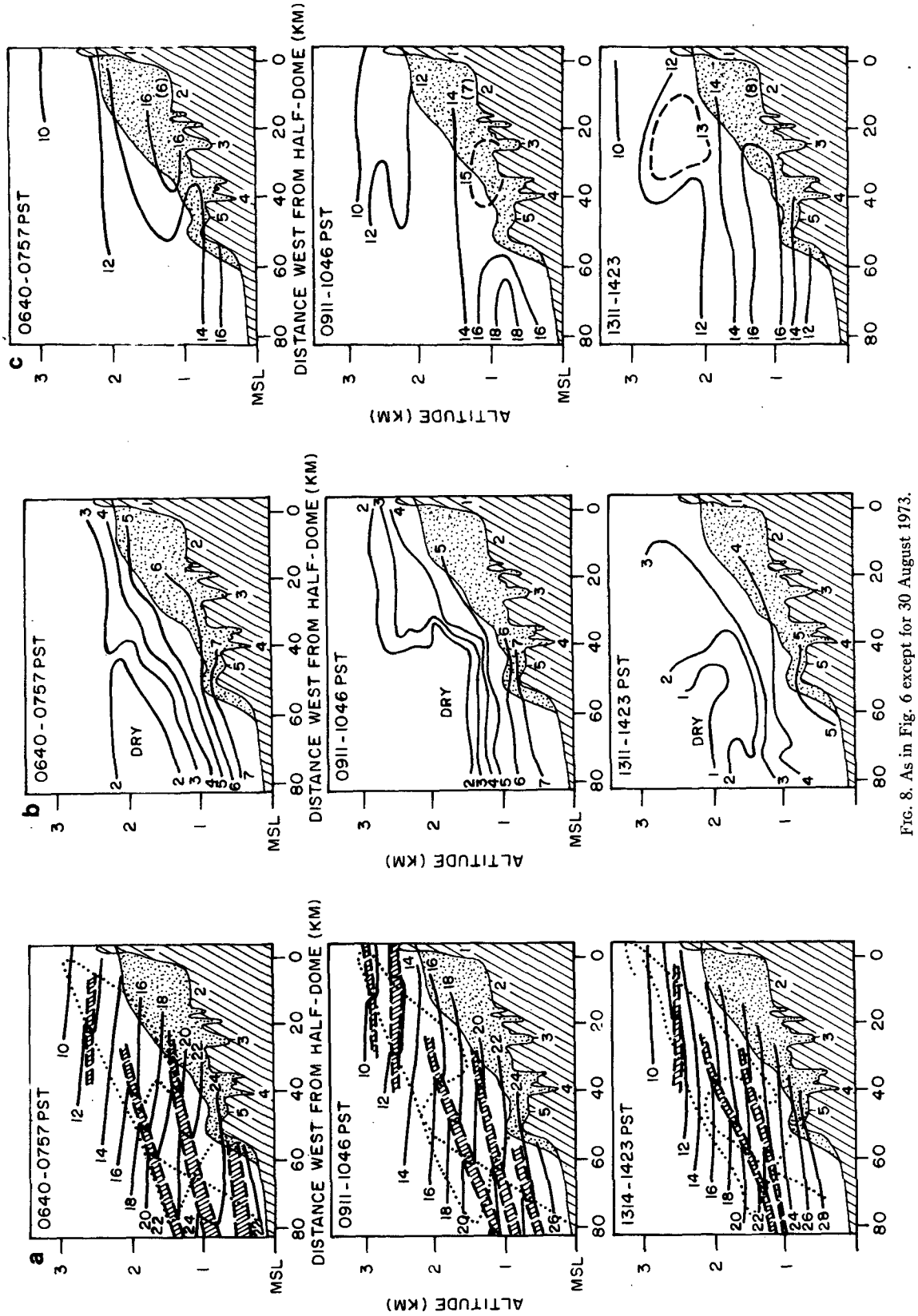


FIG. 8. As in Fig. 6 except for 30 August 1973.

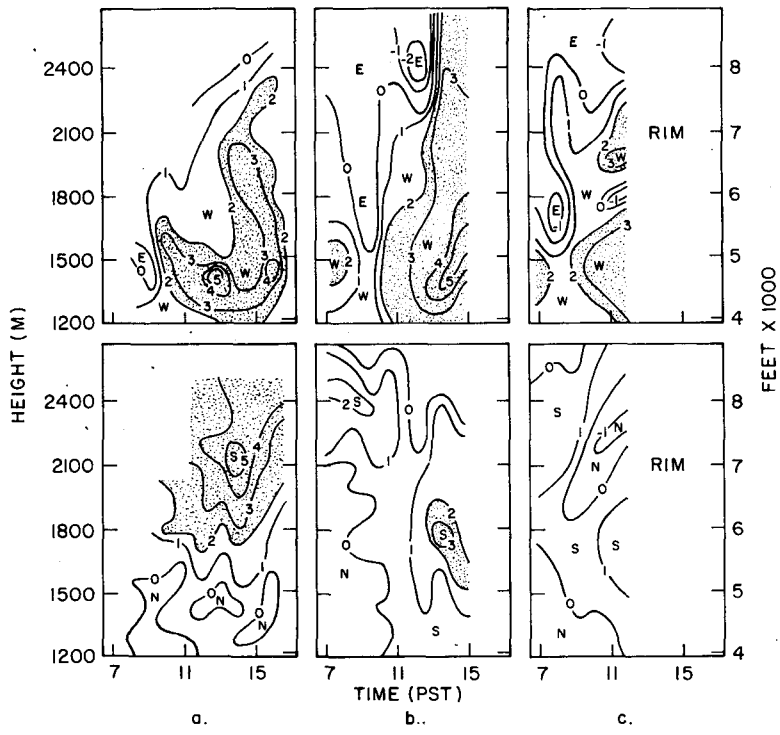


FIG. 9. Time-height cross sections of single theodolite pibal wind measurements near El Capitan Meadows for (a) 26 July, (b) 29 August and (c) 30 August, respectively. Upper diagram shows the westerly component, lower the southerly component. Isotachs are drawn every 1 m $s^{-1}$, with west or south winds >2 m $s^{-1}$ shaded.

and thermal convection produced increased turbulence and an increasing mixed-layer depth. Note, however, that while the mixed-layer depth increased from a few hundred meters to over 1500 m and the wind speeds increased through midafternoon, the $O_3$ concentration and the thickness of the polluted layer over both the Central Valley and the lower slopes also increased. In spite of the greater dispersion conditions present on this day, the $O_3$ concentrations exceeded those measured in July both aloft and at El Capitan. We interpret the rapid rise in oxidant measured at El Capitan (8–12 pphm) between 1400 and 1500 PST as the arrival of the $O_3$ maximum detected by the aircraft just downslope of El Portal.

The data for 30 August show continued increase in total pollutants, although the maximum local con-

TABLE 4. Total particle concentrations by number ($D \gtrsim 0.3$ μm) measured during ascending (1.5 ≲altitude≲3.2 km, MSL) and descending (1.3≲altitude≲2.3 km, MSL) flight paths and the mass concentration calculated from the number-size distribution and an assumed particle density of 2 g $cm^{-3}$.

| Date | Time | Observed number concentration (particles $cm^{-3}$) | | | Calculated mass concentration (μg $m^{-3}$) | | |
|---|---|---|---|---|---|---|---|
| | | Ascent | Descent | Mean | Ascent | Descent | Mean |
| 26 Jul | Early | 235 | 375 | 328 | 107 | 104 | 109 |
| | Midday | 173 | 421 | 339 | 80 | 105 | 86 |
| | Afternoon | 220 | 341 | 281 | 134 | 37 | 83 |
| 27 Jul | Early | 111 | 278 | 195 | 45 | 67 | 55 |
| | Midday | 104 | 139 | 143 | 61 | 70 | 64 |
| 29 Aug | Early | 69 | 405 | 237 | 28 | 51 | 46 |
| | Midday | 139 | 298 | 218 | 165 | 125 | 152 |
| | Afternoon | 445 | 600 | 502 | 140 | 235 | 188 |
| 30 Aug | Early | 724 | 404 | 564 | 304 | 116 | 219 |
| | Midday | 240 | 584 | 412 | 141 | 90 | 123 |
| | Afternoon | 550 | — | — | 76 | — | — |

centrations are slightly lower than on the 29th. What is especially significant is that throughout the spatial domain of the aircraft observations the uncorrected $O_3$ mixing ratios exceed 10 pphm up to 3000 m; recalling that the true mixing ratios are the order of 25% greater at this altitude, it is quite evident that the vertically integrated total $O_3$ over the slopes is greater on this day than in any other observational period.

Examination of Table 4 reveals the same general trends in particle concentrations as those discussed above, i.e., the concentrations generally decrease with height at any time and are greater in August than in July. In addition the total particle concentration aloft decreases with time in July but increases with time of day in August. An exception to these trends was observed during the first flight on 30 August when the largest number concentration among all flights was observed on the upslope leg. This anomaly was apparently due to a dense aerosal layer at and above 2100 m which was not encountered in subsequent flights. In general, the size distribution shifts toward smaller diameters through the day as is reflected in the lack of correspondence of changes in number density and changes in mass concentrations in Table 4. As the microscopic size analysis was performed under conditions of nearly constant relative humidity the observed changes in size distribution appears to have been due to increased production of submicron particles rather than changing ambient relative humidity.

In summary it would appear that in the vicinity of Yosemite National Park, in summer, at elevation $<2000$ m, under *minimal* dispersion conditions, local anthropogenic and natural sources could cause persistent ground level oxidant concentrations of 6–8 pphm, and particle-borne sulfur concentrations the order of 0.4 $\mu$gm m$^{-3}$ ($D \gtrsim 0.3$ $\mu$m). In contrast, transport of pollutants from distance sources, associated with increased daytime ventilation and improved dispersion conditions, could result in local, short-period, near-ground oxidant concentrations in excess of 25 pphm and persistent afternoon concentrations in excess of 12 pphm at elevations up to at least 3000 m. A fourfold increase in particle-borne sulfur is also likely.

An upper limit on the average frequency of occurrence of conditions similar to those described for August can be estimated for the summer period (15 May–15 September). The shortest sequence would be one day of transition from sea breeze to stagnation conditions, two days of stagnation, transition to the sea breeze regime and two days of sea breeze, i.e., about a 6-day period. In fact, the number of sea breeze days exceeds the number of stagnation days so that a more realistic frequency of occurrence of the August conditions is less than three periods per month.

It should also be emphasized that this discussion pertains only to the lower half of the western slope of the Sierra over which the observations were made. Above these elevations, ground-level concentrations probably decrease fairly rapidly with distance upslope due to increased deep thermal convection over the upper slopes. In addition, with very weak synoptic-scale pressure gradients aloft, the upslope winds may separate from the surface before reaching the crest, if a counterflow aloft is present, thereby forming a closed vertical circulation. In this case, a significant portion of pollutants transported upslope would be advected back over the lower slopes aloft. Since pibal observations were not generally possible to these altitudes we have no conclusive evidence that these counterflows were present. However, the high pollution concentrations observed above the stable layers on 30 August plus the pattern of redistribution of water vapor with time of day suggest that counterflow aloft was present on this day and the previous day.

## 4. Concluding remarks

The data presented clearly verifies the scenario described in the Introduction, namely, that transport by the extended sea breeze circulation and the valley wind system can cause significant degradation of air quality in an area such as Yosemite due to emissions from sources up to several hundred kilometers away. While these results refer to a very specific geographical area, in which very specific meteorological conditions occur, they are illustrative of the general problem of evaluating air quality maintenance strategies and of interpreting local air quality survey data in areas where mesoscale circulations as modulated by synoptic-scale events are the major determinants of regional air pollution transport and dispersion. In other words, the "worst case" air pollution situations in areas of low emission rates are not necessarily stagnation periods but may be periods with good ventilation. Finally, it is apparent that while local emission reduction in the Yosemite Valley would preclude further degradation of air quality during local stagnation periods, as in the early morning hours and in winter, they would have limited impact on the summertime worst case situations as described here.

*Acknowledgments.* The authors wish to express their gratitude to the students who assisted in the acquisition and analysis of the field data, to Messrs. G. Weigt and R. Judkins who contributed significantly to the development and installation of the aircraft instrumentation, and to Mr. R. Cowden for his guidance in this development and for his skillful piloting of the aircraft during the study. Support for this work was provided by the Agricultural Experiment Station and the CASE[2] Institute of the University of California, which is gratefully acknowldged.

[2] Council for the Advanced Study of the Environment.

## REFERENCES

Angell, J. K., D. H. Pack, G. C. Holzworth and C. R. Dickson, 1966: Tetron trajectories in an urban atmosphere. *J. Appl. Meteor.*, **5**, 565–572.

Ayers, H., 1961: On the dissipation of drainage wind systems in valleys in morning hours. *J. Meteor.*, **18**, 560–563.

Baskett, R. L., 1976: Air quality determinations in the Yosemite Valley California Airshed. M.S. thesis, Atmos. Sci. Dept., University California, Davis, 140 pp.

Cramer, O. P., and R. E. Lynott, 1961: Cross section analysis in a study of wind flow over mountainous terrain. *Bull. Amer. Meteor. Soc.*, **42**, 693–702.

Fleagle, R. G., 1950: A theory of air drainage. *J. Meteor.*, **7**, 227–232.

Fosberg, M. A., and M. J. Schroeder, 1966: Marine air penetration in central California. *J. Appl. Meteor.*, **5**, 573–589.

Frenzel, C. W., 1962: Diurnal wind variations on central California. *J. Appl. Meteor.*, **1**, 405–412.

Gleeson, T. A., 1953: Effects of various factors on valley winds. *J. Meteor.*, **10**, 262–269.

Miller, A., and D. Ahrens, 1970: Ozone within and below the West Coast temperature inversion. *Tellus*, **22** 328–340.

Miller, P. R., M. H. McCutchan and H. P. Milligan, 1972: Oxidant air pollution in the Central Valley, Sierra Nevada Foothills, and Mineral King Valley of California. *Atmos. Environ.*, **6**, 623–633.

Schroeder, M. J., 1961: Down canyon afternoon winds. *Bull. Amer. Meteor. Soc.*, **42**, 527–542.

——, M. A. Fosberg, O. P. Cramer and C. A. O'Dell, 1967: Marine air invasion of the Pacific Coast: A problem analysis. *Bull. Amer. Meteor. Soc.*, **48**, 802–808.

Schultz, H. B., 1974: Mesoclimatic wind patterns and their application for abatement of air pollution in the central California valley. California Air Resources Board, Project Clean Air, Rep. No. 111, 53 pp.